SERBIAN JOURNAL OF ELECTRICAL ENGINEERING
Vol. 18, No. 3, October 2021, 303-320

UDC: 621.314.26 **DOI: https://doi.org/10.2298/SJEE2103303B**

Optimal Design of Minimal Footprint High Frequency Transformer

Jeyapradha Ravichandran Banumathy[1], Rajini Veeraraghavalu[1]

Abstract: Transformer design procedure may vary essentially in respect of the transformer type and its operating frequency (ranging between 50/60 Hz and a few megahertz). This paper presents a simple and straightforward method based on the optimal choice of core geometry of a high frequency transformer (HFT) used in Solid State Transformer (SST) applications. The core of SST is the HFT which largely influences its size and overall performance. The proposed design procedure for HFT focuses on optimizing the core geometry coefficient (in cm^5) with a constraint inflicted on loss density. The core geometry coefficient has direct impact on the regulation and copper loss and the procedure results in a robust overall design with minimal footprint. Also, the procedure intends to bring all the operating parameters like regulation, losses and temperature rise within permissible limits while retaining desired efficiency. Thus an energy-efficient design is achieved with minimal footprint. The optimization procedure is implemented using recently developed Moth-flame Optimization (MFO) algorithm. The results of the MFO algorithm are compared with the well-established PSO technique. An experimental prototype is built to validate the findings.

Keywords: Optimization, Medium Frequency transformer, Bio-inspired algorithm, Solid State Transformer, Isolated DC-DC Converter.

1 Introduction

In the global pursuit for accomplishing green environment, research efforts are motivated to modernize major components of the electric utility system. One such effort is the development of Solid State Transformer as a potential alternative to conventional distribution transformer (CDT). Unlike CDT, SST is pollution-free and hence considered as a milestone invention to meet the needs of sustainable energy future. SST has been drawing huge attention as prospective component of utility distribution systems in recent years, thanks to its embedded intelligence and ability to provide additional services besides energy transformation and isolation.

[1]Department of Electrical and Electronics Engineering, SSN College of Engineering, Rajiv Gandhi Salai, Kalavakkam, Chengalpattu District, Tamilnadu, India- 603110.
E-mails: jeyapradharb@ssn.edu.in; rajiniv@ssn.edu.in

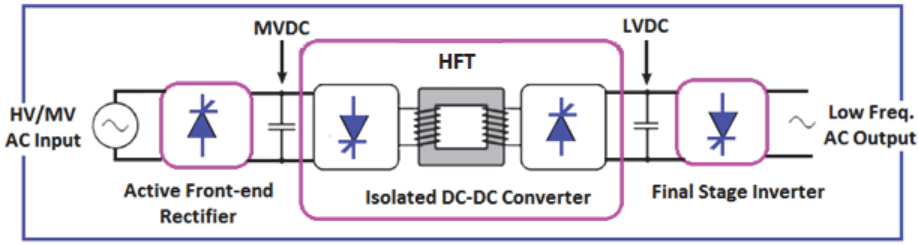

Fig. 1 – *Typical Three-stage SST architecture.*

The nucleus of the three-stage SST system shown in Fig. 1 is the medium frequency isolated dc-dc converter which serves as an interface between medium voltage ac and low voltage ac/dc grids [1 – 3]. The converter and hence the high frequency transformer (HFT) design greatly influences the performance as well as footprint of the SST. Operation at high/medium frequencies though results in high power densities and reduced size and weight for the HFT, it also leads to increased core loss, magnetic saturation and temperature rise at high voltages [4]. Therefore choice of magnetic material becomes crucial to attain high power densities and efficiencies. Significant attention must be paid to issues related to thermal management as well, in order to overcome the increased loss density with reduced footprint. Further, wire selection must be carefully done because skin and proximity effects in the windings become more pronounced at high frequencies. Thus a cumulative design approach is needed for HFT such that all the challenges concerned with high frequency operation are overcome simultaneously offering desired efficiency and regulation.

2 Literature Background

Many approaches to high/medium frequency transformer (HFT/MFT) design for various applications were reported in the past. Previously, HFT design for switching power supplies were developed [5 – 8]. Later, efforts were made to design HFT with minimal size and weight for high power isolated DC-DC converters employed in distribution grids. This was deemed appropriate for offshore wind installations as reported in [4] where a 500 Hz transformer was shown to be 1/3rd the weight of its equivalent 50 Hz one. The prospects of deploying HFTs in traction applications were also discussed in the past [9]. A 350 kW/8kHz transformer as a substitute for a 16.7 Hz transformer was designed for on-board railway vehicles [10] and was proved to have a significant volume reduction. Recently, attempts on design of high/medium frequency transformers for SST applications have been widely reported [11 – 14]. All the aforementioned research endeavours have focused chiefly on the benefits of utilizing higher frequencies, rather than on the design aspects and optimization of

such a transformer. A new procedure based on brute-force approach for design optimization of MFT for SST applications has been documented in [15]. While the procedure seems really interesting, the generation of all feasible solutions is really cumbersome and the data processing is time consuming.

Further scrutiny of literature divulges information on research efforts undertaken to optimize the HFT design. Typical attempts on optimization concentrated on a factor named area product by which the amount of power handled by the core is established [6, 16]. Nevertheless, the proposed procedure has not been validated for high power, high frequency applications. A design optimization of HFT with high isolation requirements and thermal management based on round litz wires [17] has been discussed in [18]. Also, optimization with emphasis on thermal and insulation design [19] and maximizing the power density by accounting for tuned leakage inductance [20, 21] were documented in the past. A HFT optimization design to exploit the utilization of the transformer to achieve high power density with minimum transformer loss has been reported in [22]. Recently, a medium frequency transformer design has been proposed based on open-source optimization framework where the magnetic field calculation is done by a built-in FEM solver [23, 24].

Thus, several of the challenges pertaining to HFT/MFT design mentioned earlier have been addressed individually and solutions provided in the past by researchers across the globe. However, a comprehensive design taking into account all the significant challenges are rarely not yet documented in literature. Therefore, further investigations are needed in order to achieve high power density, better regulation along with good thermal management while retaining high efficiency for the HFT. Additionally, all the recorded research work have centered around either single or multi-objective optimization with or without constraints along with a method to check limits on operating parameters prior to arriving at an optimal solution to the problem. This is a lengthy process because whenever an operating parameter violates the bounds, the algorithm hunts for a new optimal solution that satisfies the limits.

With all the above concerns in mind, the work reported in [25] was intended to develop a novel optimization procedure for the design of HFT which takes into account the core geometry coefficient (in cm^5) [6] with a constraint inflicted on loss density. The method proposed confines all the working parameters within expected limits while preserving desired efficiency. Further, the method resulted in a minimal footprint for the HFT. However, a laboratory prototype of the HFT was not developed to support the claims. This paper on the other hand validates the findings by constructing a laboratory prototype of the converter with the HFT before and after optimization. The efficiency of the converter with HFT before and after optimization were also compared for better understanding.

3 MFO Algorithm

Bio-inspired optimization algorithms are finding extensive applications in solving real and composite engineering design problems over the past few years [26, 27]. Significant attention is being given to these algorithms owing to complex and dynamic nature of the problems, wide range of possible multidimensional solutions, and challenges related to partial and/or limited information for arriving at an optimal solution [28, 29]. Adequate literature is available in this domain with major focus on Genetic Algorithms (GA), Ant Colony Optimization (ACO) and Particle Swarm Optimization (PSO). However, in recent times, number of new algorithms are developed mimicking the behaviour of bio-organisms, namely, Whale Optimization algorithm (WOA), Dragon Fly (DA) algorithm, Ant-Lion Optimization (ALO), Grey-Wolf Optimizer (GWO) and so on. One such algorithm is the Moth-Flame Optimization (MFO) algorithm proposed in [30]. The MFO algorithm is developed based on the tendency of moths to adopt transverse orientation for their navigation towards moonlight. However they are diverted by artificial lights and end up following deadly spiral paths. This activity of moths is mathematically modeled for optimization as shown in Fig. 2.

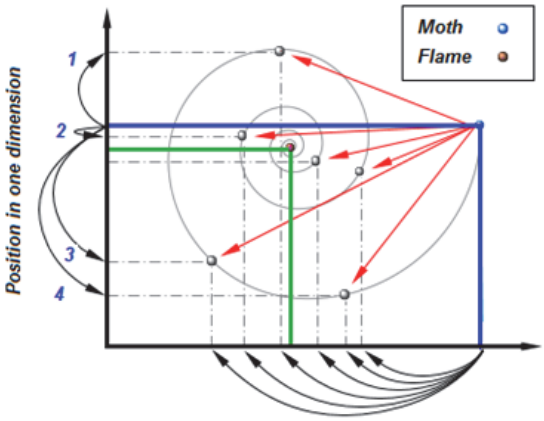

Fig. 2 – *Mathematical modeling of MFO algorithm* [31].

This paper is aimed at using the MFO algorithm for high frequency transformer (HFT) design problem. Initially, optimization problems with respect to transformer design have been solved using GA [8, 31]. Later, Bacterial Foraging Algorithm (BFA) [32] and PSO algorithm [33] have been applied to solve these problems. In this paper, recently developed MFO algorithm which has not been applied to transformer design problem hitherto, is adopted to solve the design problem of HFT used in Solid State Transformer (SST) applications. The results are then compared with the well established PSO technique. The

proposed method for optimization is more simple and uncomplicated in comparison to the methods documented in literature. The optimal HFT is then implemented as a laboratory prototype for low power applications using isolated half-bridge converter.

4 Optimization Procedure for HFT

The step-by-step design procedure for HFT design of dc-dc converters outlined by McLyman [6] has been followed here. An isolated half-bridge converter is chosen for the design case study and the corresponding design equations are presented along with the procedure for optimization. The design inputs to the optimization problem are the power rating P_o of the isolated half-bridge converter and the input and output voltages, U_{in} and U_o respectively. Efficiency (η), % regulation (α), utilization factor (k_u) and waveform coefficient (K_W) are kept fixed. The design of HFT is normally realized for a given temperature rise. However, the design can be realized for a known % regulation, α. The α, as defined by McLyman is related to two coefficients namely, the electrical coefficient, K_{el} and the core geometry coefficient, K_{cg} given by

$$K_{el} = 0.145 k_w^{\,2} f_s^{\,2} B^2 10^{-4}, \tag{1}$$

$$K_{cg} = \frac{S}{2K_{el}\alpha}, \tag{2}$$

where S is the total apparent power in watts, f_s is the operating frequency in Hz and B is the flux density in Tesla. K_{cg} can also be expressed as

$$K_g = \frac{A_w A_e^{\,2} k_u}{L_{mt}} [\mathrm{cm}^5], \tag{3}$$

where A_W is the window area in cm^2, A_e is the effective core cross-section in cm^2 and L_{mt} is the mean length of the turn in cm. It is clear from (2) and (3) that K_{cg} affects the regulation and copper loss besides influencing the size of the magnetic components. Thus K_{cg} can be optimized to design a highly compact and efficient HFT, concurrently confining the other key design requirements like % regulation, current density in the windings, copper losses, temperature rise etc., within specified bounds.

For a given % regulation, K_{cg} is a function of two variables namely, f_s and B as noted from (1) and (2). The variation of core geometry coefficient with operating frequency and flux density is depicted in Fig. 3. In low frequency transformer design, with emf induced per turn remaining constant, increasing the operating frequency of the transformer actually reduces the peak flux density of the core and vice-versa. However the proposed design for HFT does not

necessitate constant emf/turn and hence flux density and frequency are chosen as free parameters to establish optimal core geometry.

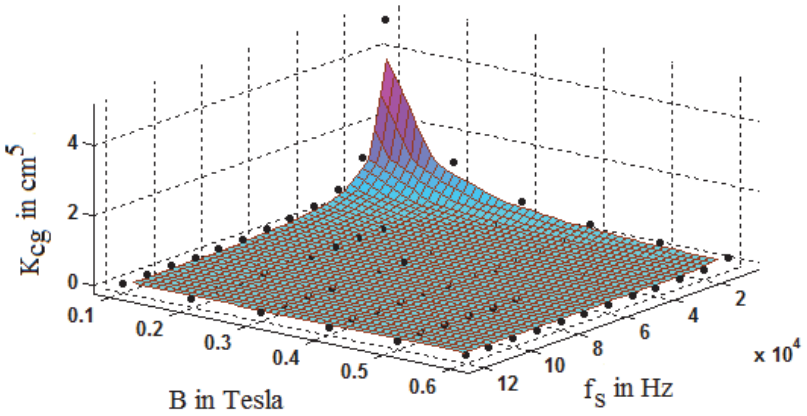

Fig. 3 – *Plot of coefficient of core geometry vs operating frequency and flux density.*

With frequency and flux density as free parameters and a constraint inflicted on specific loss, the objective function of the design optimization problem is given by:

Minimize K_{cg} such that

(i) $f_{s\min} < f_s < f_{s\max}$

(ii) $B_{\min} < B < B_{\max}$

with the constraint $W_{sp}(f_s, B) - 0.05 \times P_s < 0^{\#}$

where W_{sp} is the specific loss in W/kg and $P_s = P_o(1/\eta + 1)$ is the total apparent power in W.

 # Specific loss is assumed to be limited to 5% of total apparent power.

In the proposed optimization procedure, instead of holding *V/f* constant to eliminate over-fluxing as in the case of low frequency transformer, the operating frequency is swung across a given range together with flux density. This is because the choice of core and its dimensions are made only after seeking an optimum solution for K_{cg}.

With the best generated free parameters and the optimal value for core geometry coefficient obtained from the MFO algorithm, the appropriate choice of core material is made from the core data table corresponding to the optimal value. Generally, the core with a little higher value for K_{cg} than the optimal value is chosen to ascertain minimal copper loss. The dimensions of the selected core viz., mean length of the turn (L_{mt}), magnetic path length (L_{mp}), total weight of the core (W_{fe}), total copper weight (W_{cu}), minimum cross-sectional area of the core

(A_c), window area (A_w), area product (A_p) and overall surface area of the magnetic component (A_s) are extracted from the core data table. With these dimensions, the performance parameters of the HFT are estimated.

The number of primary turns is obtained by

$$N_{pri} = \frac{U_{pri} 10^4}{K_w B_{opt} f_{s\_opt} A_c}, \tag{4}$$

where B_{opt} and f_{s_opt} are the best fit values for flux density in Tesla and frequency in Hertz respectively and

$$U_{pri} = \frac{U_{in}}{2}\left(2D_{\max}\right) - I_{pri} R_q \tag{5}$$

is the average primary voltage in volts, D_{max} is the maximum duty cycle of the converter and R_q is the transistor resistance in ohms.

The average primary current for the half-bridge converter is given by

$$I_{pri} = \frac{2P_o}{U_{in}\eta}. \tag{6}$$

The current density in the windings in amps/cm^2 is then calculated by

$$J = \frac{P_s 10^4}{K_w K_u B_{opt} f_{s\_opt} A_p}, \tag{7}$$

where P_S is the total apparent power in watts and A_P is the area product in cm^2.

With the known value of current density, the primary wire area in cm^2 is estimated as

$$A_{wpri} = \frac{I_{pri}}{J\sqrt{2D_{\max}}}. \tag{8}$$

A proper choice of wire is made from the wire table with the required wire area. If the wire area from the table is in excess of 10% of the required wire area, then the next smallest size is chosen.

Upon selecting appropriate wire for the design, the primary winding resistance and hence primary copper losses are estimated. The primary winding resistance in ohms,

$$R_{pri} = L_{mt}\left(N_{pri}\right)\left(\frac{\mu\Omega}{\text{cm}}\right)10^{-6}, \tag{9}$$

where μΩ/cm is the specific resistance of the chosen wire. The primary copper losses in watts are given by

$$P_{cup} = \frac{I_{pri}^{2}}{2D_{\max}} R_{pri} . \tag{10}$$

The number of secondary turns on each side of the centre tap (if any) is then calculated using the equation below:

$$N_{sy} = \frac{N_{pri}\left(U_o + U_d\right)}{U_{pri}}\left(1 + \frac{\alpha}{100}\right), \tag{11}$$

where U_d is the diode voltage drop. Similar to the primary winding design, the secondary wire area (A_{wsy}), secondary winding resistance (R_{sy}) and hence secondary copper losses (P_{cus}) are estimated. The new value of window utilization factor is then updated as

$$K_{u\,new} = \frac{N_{pri} S_n A_{wire\_p} + N_{sy} S_n A_{wire\_s}}{A_w}, \tag{12}$$

where A_{wire_p} and A_{wire_s} are the selected wire areas from the wire table for the primary and secondary windings respectively. S_n represents the number of strands of primary and secondary wires given by the ratio of actual wire area to the bare wire area obtained from the wire table. Following K_u, the % regulation α is also updated with the new value

$$\alpha_{new} = \frac{P_{cu}}{P_o} 100, \tag{13}$$

where P_{cu} is the sum of primary and secondary copper losses. The new value of flux density is now calculated as

$$B_{new} = \frac{U_{pri} 10^4}{K_w f_{s\_opt} A_c N_{pri}} \tag{14}$$

and the corresponding loss density is given by

$$W_{sp} = 3.18 \times 10^{-4} (f_{s\_opt})^{1.51} (B_{new})^{2.747} . \tag{15}$$

Subsequently, the core losses in watts are estimated to be

$$P_{fe} = W_{sp} (W_{fe}) 10^{-3} . \tag{16}$$

The final stage of the design includes computation of loss density (W/cm^2) and the resultant temperature rise in °C.

$$\lambda = \frac{P_{tot}}{A_s}, \tag{17}$$

where P_{tot} is the sum of core and copper losses. The temperature rise is given by

$$\Delta T = 450(\lambda)^{0.826} . \tag{18}$$

5 Optimization Results and Discussion

The optimization procedure and the parameter calculation for HFT described in the previous section are presented as a simple flow diagram in Fig. 4. A single dc-dc converter module is considered for evaluating the case study whose specifications are listed in **Table 1**. For SST applications, several such modules can be connected in parallel at the low voltage side (LVDC link) and in series at the high/medium voltage side (HVDC/MVDC link) as per requirement as shown in Fig. 5. The fixed parameters assumed for the case study under consideration is presented in **Table 2**.

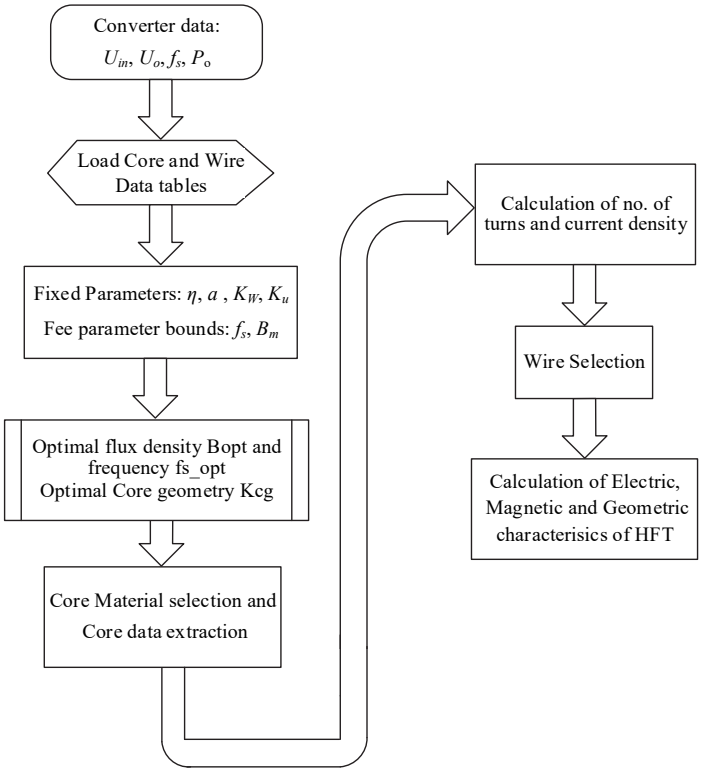

Fig. 4 – *Flowchart for HFT optimization.*

Table 1
Design specifications of a single converter module.

Design Parameters	Specification
Output Power, P_o (W)	250
Nominal Input Voltage, U_{in} (V)	100
Output Voltage, U_o (V)	75
Output Current, I_o (A)	3.33

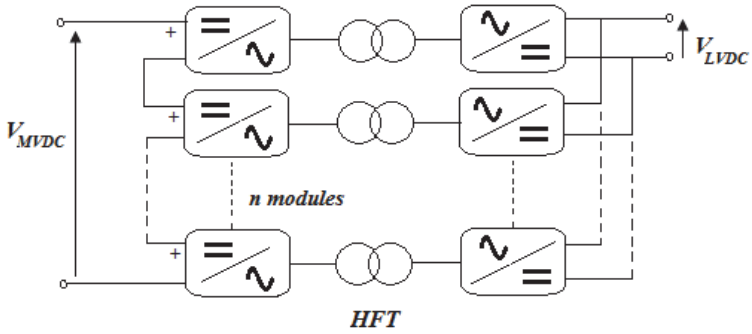

Fig. 5 – *Modular arrangement of isolated DC-DC converters.*

Table 2
Fixed parameters for optimization.

% Efficiency, η	96
% Regulation, α	0.6
Window utilization factor, K_u	0.4
Waveform coefficient, K_w (for square wave)	4.0

The free parameters, namely, f_S and B are varied over a wide range within expected limits to find the best optimal value for K_{cg}. The operating frequency is varied between 10 kHz and 75 kHz and the maximum flux density between 0.1 T and 0.6 T. The saturation flux density of the material employed for the core is taken as the upper limit. However, 10 – 20% margin of safety is allowed to keep away from saturation. As ferrite core is chosen for the design case study, the upper limit for B is fixed at 0.6 T. The choice of ferrite core can be attributed to the fact that they exhibit lower core losses (> 20 kHz) and are available in an assortment of geometric shapes.

In the direct design procedure for HFT, the choice of 15 kHz for frequency and 0.45T for the corresponding flux density is arbitrary. The core geometry corresponding to the chosen values of frequency and flux density is obtained as 0.05164 cm^5. After optimization using MFO, the best values for free parameters are established as 50 kHz and 0.1609 T and the optimal core geometry is 0.03635 cm^5. A relative comparison of the performance of HFT before and after optimization is presented in **Tables 3** and **4**. The core data for the calculated value of K_g before optimization and that for the optimal value of K_g are listed in **Table 3**. The look up table for the core data is generated with the details obtained from Magnetics®, the leading magnetic component suppliers. F-type ferrite material has been chosen as they are very much suitable for converter transformers with

reasonably good permeability, low losses and high saturation. **Table 4** presents the electric, magnetic and geometric characteristics of the HFT before and after optimization.

Table 3
Core data before and after optimization.

Core data	Before optimization	After optimization	Core data	Before optimization	After optimization
K_{cg} (cm^5)	0.05164	0.03635	W_{cu} (gm)	36.39	19.96
Core material part No.	EE 37	EE 44	A_c (cm^2)	0.821	1.01
L_{mp} (cm)	6.94	5.19	A_w (cm^2)	1.5396	0.7226
L_{mt} (cm)	6.646	7.77	A_p (cm^4)	1.264	0.7298
W_{fe} (gm)	33.09	26	A_s (cm^2)	45.39	41.34

Table 4
Electric, magnetic and geometric characteristics of HFT before and after optimization.

Transformer characteristics	Before optimization	After optimization	Transformer characteristics	Before optimization	After optimization
J (A/cm^2)	383.86	557.81	B_{new} (T)	0.4482	0.1632
R_{pri} (Ω)	0.0292	0.0672	N_{pri}	21	13
R_{sy} (Ω)	0.0487	0.119	N_{sy}	35	23
P_{cu} (W)	0.7569	1.857	A_{wpri} (cm^2)	0.007	0.005
P_{fe} (W)	2.347	0.7084	A_{wsy} (cm^2)	0.006	0.004
P_{tot} (W)	3.104	2.565	S_n	1	2
λ (W/cm^2)	0.06834	0.0621	W_{sp} (W/kg)	70.93	27.25
α_*new* (%)	0.2949	0.7234	ΔT (°C)	49.078	45.29

It is inferred from **Table 3** that optimizing the core geometry results in reduction of both core and copper weights. Though an increase in core cross-sectional area is observed, the window area is very much reduced and hence the area product. Thus a minimal footprint is achieved for HFT. Analyzing the data presented in **Table 4**, it is understood that despite an increase in copper losses, the total losses are reduced roughly by 20% following optimization. The specific loss is limited to 5% of the total apparent power as per the problem statement. The new value of regulation is 0.72% which is well within desired limits. Also, the temperature rise is limited to 45°C after optimization. This proves the effectiveness of the proposed optimization procedure.

Table 5
Comparison of Performance of MFO and PSO algorithms.

Optimization algorithm	Operating frequency, f_{s_best} (kHz)	Maximum flux density, B_{best} (T)	Coefficient of core gegometry, K_{cg_opt} (cm^5)	Average overall computational time (s)	Average no. of iterations for convergence
MFO	50	0.1609	0.03635	0.7939	23
PSO	49.88	0.1611	0.03642	0.4039	66.6

A comparative evaluation of the MFO algorithm with the PSO technique is made and the results presented in **Table 5**. The comparison is carried out for the test case presented in **Table 1**. Both the algorithms are compared based on identical search agents (equal to 100). The convergence speed and the number of iterations required for convergence are averaged over 10 successive runs. For the proposed optimization problem, it is discerned from the table that both the algorithms return identical optimal solution though they differ in speed of computation, consistency in producing solutions in consecutive runs and convergence.

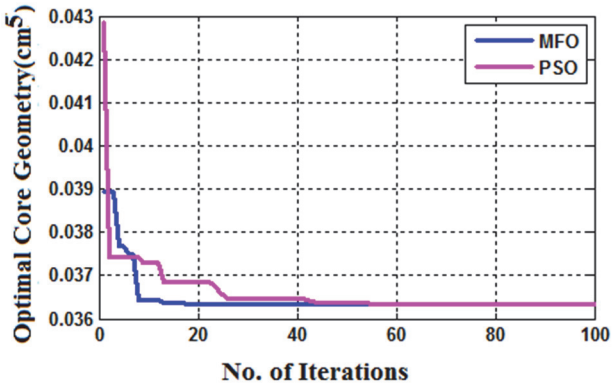

Fig. 6 – *Plot of convergence for MFO and PSO algorithms.*

Fig. 6 shows the convergence of the MFO and PSO algorithms plotted for case study under consideration. It is clear from the plot that MFO converges quickly than PSO. However, it is observed from **Table 5** that though MFO is quick to converge compared to PSO algorithm, the relative computational time is the least with PSO. This is because the computational time per iteration is the least with the PSO algorithm. Additionally, MFO is found to be more consistent in producing the optimal solution than PSO.

6 Experimental Validation and Results

The proposed optimization procedure for HFT discussed in the preceding sections is validated with an experimental setup. The HFTs before and after optimization are tested for their performance by incorporating them into the Half-bridge converter circuit and the results are compared to highlight the benefits of the proposed optimization procedure. Since the key objective here is the design optimization of HFT, a simple half-bridge dc-dc converter topology is chosen for unidirectional and Modular SST applications. Nevertheless, the design optimization can be carried out with any dc-dc converter topology that is deemed appropriate for a specific application.

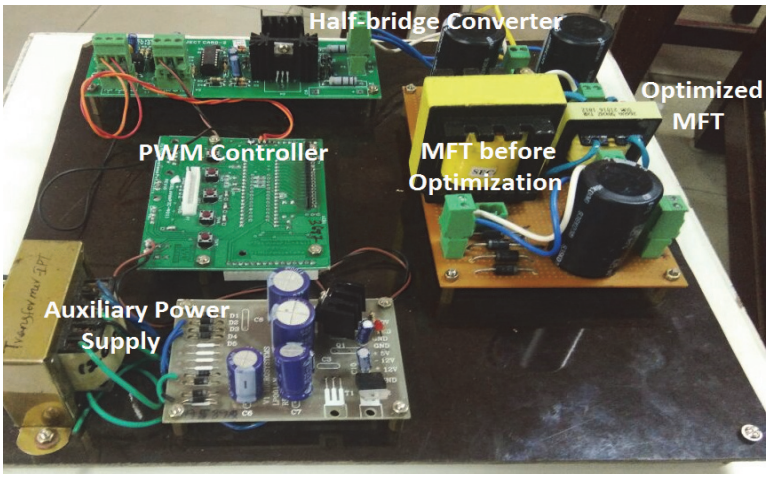

Fig. 7 – *Experimental prototype of Half- bridge converter with HFT.*

Table 6
Ratings of major components of the prototype.

Component	Part No.	Ratings
MOSFET	IRFP840	500V, 8A, 0.85Ω
Diode	MUR 440	400V, 4A
Capacitors	-	330μF, 450V
Optocoupler IC	A4506	-
MOSFET Driver	IRS2110	500V dc offset, 10-20V o/p, 130ns &120ns $t_{on/off}$
PWM Controller	dsPIC30F4011	16 bit controller with 6 PWM output channels
Resistive Load	-	25Ω
HFT1	EE375	Turn's ratio: 1.4, 15 kHz
HFT2	EE44008	Turn's ratio: 1.4, 50 kHz

A single 250 W Half-bridge converter circuit is built with provisions for plugging in the HFTs before and after optimization as shown in Fig. 7. A 100 V dc input is fed to the converter through bridge rectifier module and the results are recorded by plugging in the HFTs one after the other. The ratings of major components are presented in **Table 6**. The results obtained are presented below in Figs. 8 – 10.

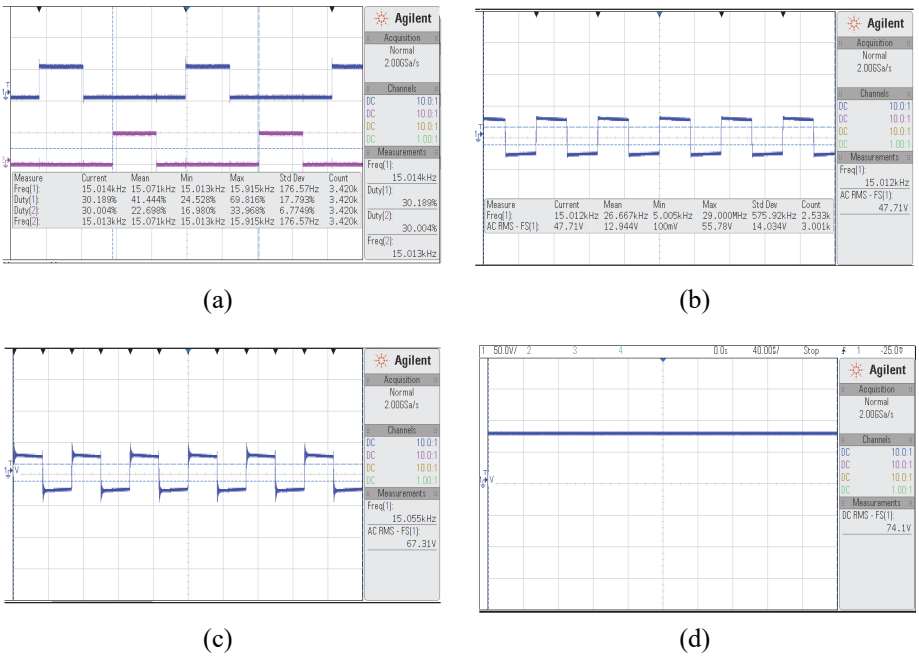

(a) (b)

(c) (d)

Fig. 8 – *Results from Prototype with HFT before Optimization* (a) *PWM pulses to the MOSFETs* (b) *Primary voltage of HFT* (c) *Secondary voltage of HFT* (d) *Output voltage of the converter.*

Fig. 8 depicts the performance of Half-bridge converter with HFT before optimization. The operating frequency of the HFT is 15 kHz. The primary and secondary voltages of the HFT are observed to be 47.71 V and 67.31 V respectively. The converter output voltage is 74.1 V. The dc current drawn at the source is measured to be 2.4 A. The performance of Half bridge converter with HFT after optimization is illustrated in Figs. 9 and 10. The HFT operates at 50 kHz and the primary and secondary voltages are found to be 49.54 V and 69.79 V respectively. The converter output voltage is found to be 74.6 V and input dc current is measured to be 2.35 A. The efficiencies of the converter with the HFT before and after optimization are presented in **Table 7**.

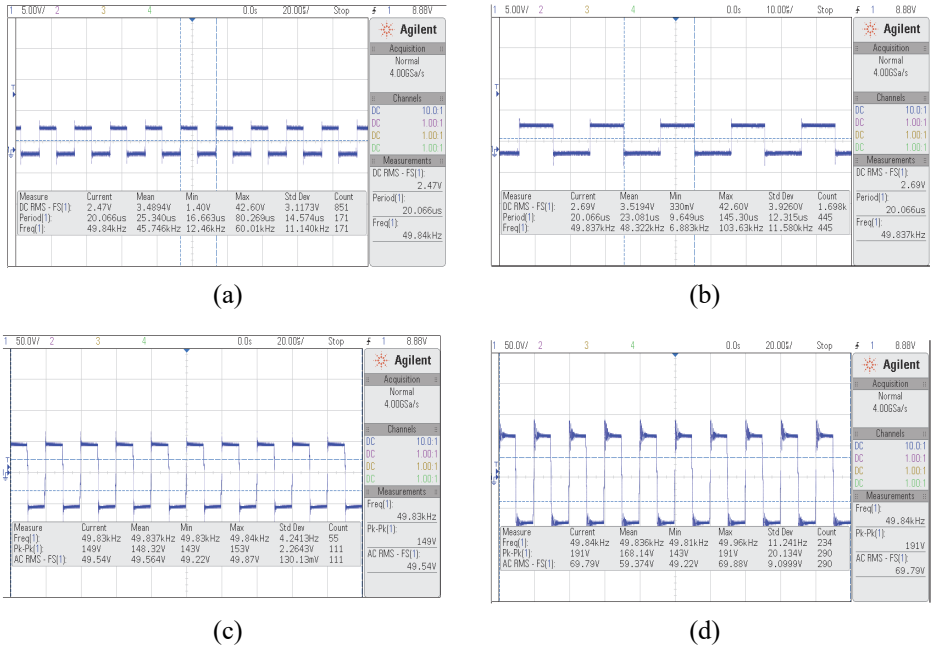

(a) (b)

(c) (d)

Fig. 9 – *Results from Prototype with HFT after Optimization*
(a) *PWM pulses to the MOSFET1* (b) *PWM pulses to the MOSFET2*
(c) *Primary voltage of HFT* (d) *Secondary voltage of HFT.*

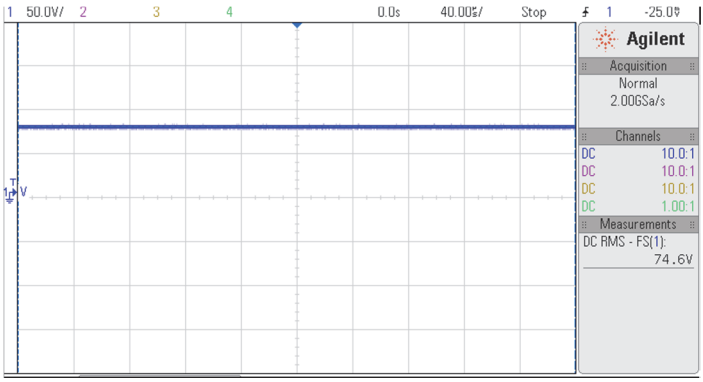

Fig. 10 – *Output Voltage of the Converter after Optimization.*

Table 7
Efficiency of Half-bridge Converter.

Half-Bridge Converter with HFT	**% Efficiency**
Before Optimization	91.50
After Optimization	94.73

It is observed that the converter with the optimized HFT produces better results for the given specifications even with a reduced footprint. This proves the effectiveness of the proposed optimization procedure.

7 Conclusion

A simple and robust single-objective design optimization procedure for HFTs employed in modular SST applications was described in this paper. The key purpose was to optimize the core geometry coefficient with a constraint imposed on specific loss in such a way that the design procedure yields a more compact and efficient HFT with all operating parameters under desirable limits. MFO algorithm was applied to solve the proposed optimization problem and its performance was compared with the well-established PSO algorithm. It was inferred that MFO exhibited relatively high speed of convergence whereas PSO required relatively low computational time. An experimental prototype of Half-bridge converter has been developed with the designed HFT and the results established the success of the proposed optimization procedure.

8 Acknowledgment

This work was supported by the All India Council for Technical Education (AICTE) [File No. 828/RIFD/RPS/POLICY-1/2016-17 dated 2nd August 2017].

9 References

[1] G. Ortiz, M. Leibl, J.W. Kolar, O. Apeldoorn: Medium Frequency Transformers for Solid-State-Transformer Applications - Design and Experimental Verification, Proceedings of the 10th IEEE International Conference on Power Electronics and Drive Systems (PEDS), Kitakyushu, Japan, April 2013, pp. 1285 – 1290.

[2] A. Shri: A Solid-State Transformer for Interconnection between the Medium- and the Low-Voltage Grid, MSc. Thesis, Faculty of Electrical Engineering, Mathematics and Computer Science, Delft University of Technology, Delft, 2013.

[3] R.J. Garcia Montoya, A. Mallela, J.C. Balda: An Evaluation of Selected Solid-State Transformer Topologies for Electric Distribution Systems, Proceedings of the IEEE Applied Power Electronics Conference and Exposition (APEC), Charlotte, USA, March 2015, pp. 1022 – 1029.

[4] S. Meier, T. Kjellqvist, S. Norrga, H.- P. Nee: Design Considerations for Medium-Frequency Power Transformers in Offshore Wind Farms, Proceedings of the 13th European Conference on Power Electronics and Applications, Barcelona, Spain, September 2009, pp. 1 – 12.

[5] N.R. Coonrod: Transformer Computer Design Aid for Higher Frequency Switching Power Supplies, IEEE Transactions on Power Electronics, Vol. PE-1, No. 4, October 1986, pp. 248 – 256.

[6] C.W.T. McLyman: Designing Magnetic Components for High Frequency DC-DC Converters, Kg Magnetics Inc., San Marino, Ca, 1993.

[7] A.I. Pressman: Switching Power Supply Design, 2nd Edition, McGraw-Hill, New York, San Francisco, 1997.

[8] K.S. Rama Rao, L.Y. Lei, S. Taib, S. Masri: Design Optimization of a High-Frequency Power Transformer for a Switching Power Supply by Genetic Algorithms Approach, Open Access Repository of USM Research and Publication, 2004, pp. 1 – 7.

[9] L. Heinemann: An Actively Cooled High Power, High Frequency Transformer with High Insulation Capability, Proceedings of the 17th Annual IEEE Applied Power Electronics Conference and Exposition (APEC), Dallas, USA, March 2002, pp. 352 – 357.

[10] M. Steiner, H. Reinold: Medium Frequency Topology in Railway Applications, Proceedings of the European Conference on Power Electronics and Applications, Aalborg, Denmark, September 2007, pp. 1 – 10.

[11] Y. Du, S. Baek, S. Bhattacharya, A.Q. Huang: High-Voltage High-Frequency Transformer Design for a 7.2kV to 120V/240V 20kVA Solid State Transformer, Proceedings of the 36th Annual Conference on IEEE Industrial Electronics Society (IECON), Glendale, USA, November 2010, pp. 493 – 498.

[12] H. Yang, X. Wang, G. Wang: Design of Electronic Transformer Used in a Proposed Circuit Topology for PET, Proceedings of the Asia-Pacific Power and Energy Engineering Conference, Shanghai, China, March 2012, pp. 1 – 4.

[13] X. She, X. Yu, F. Wang, A.Q. Huang: Design and Demonstration of a 3.6kV–120V/10KVA Solid State Transformer for Smart Grid Application, IEEE Transactions on Power Electronics, Vol. 29, No. 8, August 2014, pp. 3982 – 3996.

[14] A.M. Elrajoubi, S.S. Ang: High-Frequency Transformer Review and Design for Low-Power Solid-State Transformer Topology, Proceedings of the IEEE Texas Power and Energy Conference (TPEC), College Station, USA, February 2019, pp. 1 – 6.

[15] M. Mogorovic, D. Dujic: Medium Frequency Transformer Design and Optimization, Proceedings of the International Exhibition and Conference for Power Electronics, Intelligent Motion, Renewable Energy and Energy Management (PCIM Europe 2017), Nuremberg, Germany, May 2017, pp. 1 – 8.

[16] S. Farhangi, A.- A.S. Akmal: A Simple and Efficient Optimization Routine for Design of High Frequency Power Transformers, Proceedings of the 8th European Conference on Power Electronics and Applications (EPE 1999), Lausanne, Switzerland, September 1999, pp. 1 – 9.

[17] S. Arslan, I. Tarimer, M.E. Güven: Investigation of Current Density, Magnetic Flux Density, and Ohmic Losses for Single-Veined, Litz and Foil Structured Conductors at Different Frequencies, Pamukkale University Journal of Engineering Sciences, Vol. 19, No. 5, May 2013, pp. 195 – 200.

[18] G. Ortiz, J. Biela, J.W. Kolar: Optimized Design of Medium Frequency Transformers with High Isolation Requirements, Proceedings of the 36th Annual Conference on IEEE Industrial Electronics Society (IECON 2010), Glendale, USA, November 2010, pp. 631 – 638.

[19] P. Shuai, J. Biela: Design and Optimization of Medium Frequency, Medium Voltage Transformers, Proceedings of the 15th European Conference on Power Electronics and Applications (EPE 2013), Lille, France, September 2013, pp. 1 – 10.

[20] M.A. Bahmani: Design and Optimization of HF Transformers for High Power DC-DC Applications, BSc Thesis, Chalmers University of Technology, Goteborg, Sweden, 2014.

[21] M.A. Bahmani, T. Thiringer, M. Kharezy: Design Methodology and Optimization of a Medium Frequency Transformer for High Power DC-DC Applications, Proceedings of the IEEE Applied Power Electronics Conference and Exposition (APEC), Charlotte, USA, March 2015, pp. 2532 – 2539.

[22] S. Guo, P. Liu, L. Zhang, A.Q. Huang: Design and Optimization of the High Frequency Transformer for a 800V/1.2MHz SiC LLC Resonant Converter, Proceedings of the IEEE

Energy Conversion Congress and Exposition (ECCE), Cincinnati, USA, October 2017, pp. 5317 – 5323.

[23] T. Orosz, D. Panek, P. Karban, R.A.H. de Oliveira, J.M. Pina: Medium Frequency Transformer Design with Artap Framework, Proceedings of the 27th International Workshop on Electric Drives: MPEI Department of Electric Drives 90th Anniversary (IWED), Moscow, Russia, January 2020, pp. 1 – 4.

[24] S. Arslan, I. Tarimer, M.E. Güven, S.A. Oy: A Medium Frequency Transformer Design for Spot Welding Machine Using Sizing Equation and Finite Element Analysis, Engineering Review, Vol. 40, No. 3, May 2020, pp. 42 – 51.

[25] J.R. Banumathy, V. Rajini: High Frequency Transformer Design and Optimization using Bio-inspired algorithms, Applied Artificial Intelligence, Vol. 32, No.7-8, August 2018, pp. 1 – 20.

[26] X.- S. Yang: Review of Metaheuristics and Generalized Evolutionary Walk Algorithm, International Journal of Bio-Inspired Computation, Vol. 3, No. 2, May 2011, pp. 77 – 84.

[27] A. Gogna, A. Tayal: Metaheuristics: Review and Application, Journal of Experimental & Theoretical Artificial Intelligence, Vol. 25, No. 4, May 2013, pp. 503 – 526.

[28] X.- S. Yang: Nature-Inspired Metaheuristic Algorithms, 2nd Edition, Luniver Press, 2010.

[29] A. Kumar Kar: Bio Inspired Computing – A Review of Algorithms and Scope of Applications, Expert Systems with Applications, Vol. 59, October 2016, pp. 20 – 32.

[30] S. Mirjalili: Moth-Flame Optimization Algorithm: A Novel Nature-Inspired Heuristic Paradigm, Knowledge-Based Systems, Vol. 89, November 2015, pp. 228 – 249.

[31] V. Christopher, D. Olivier, L. Jacques: A Computer-Aided Design Tool Dedicated to Isolated DC-DC Converters based on Multiobjective Optimization Using Genetic Algorithms, COMPEL - The International Journal for Computation and Mathematics in Electrical and Electronic Engineering, Vol. 31, No. 2, March 2012, pp. 583 – 603.

[32] S. Subramanian, S. Padma: Optimization of Transformer Design Using Bacterial Foraging Algorithm, International Journal of Computer Applications, Vol. 19, No. 3, April 2011, pp. 52 – 57.

[33] A.A. Adly, S.K. Abd-El-Hafiz: A Performance-Oriented Power Transformer Design Methodology Using Multi-Objective Evolutionary Optimization, Journal of Advanced Research, Vol. 6, No. 3, May 2015, pp. 417 – 423.